J. Adhesion Sci. Technol., Vol. 18, No. 15-16, pp. 1815–1831 (2004)

Also available online - www.vsppub.com

Investigation of surface molecular orientation of poly(dimethylsiloxane-co-diphenylsiloxane)-modified poly(amic acid) films using dynamic contact angle measurements, NEXAFS and XPS

JIN HO KANG [1], KILWON CHO [1], JIN KON KIM [1], CHAN EON PARK [1,*], SUNG-JIN UHM [2] and BHANU BHUSAN KHATUA [2]

[1] *Department of Chemical Engineering, Division of Electrical Computer Engineering, Polymer Research Institute, Pohang University of Science and Technology, Pohang 790-784, South Korea*
[2] *Polymer Research Institute, Pohang University of Science and Technology, Pohang 790-784, South Korea*

Received in final form 28 October 2004

Abstract—Since poly(dimethylsiloxane)-modified poly(amic acid) was not wetted by the photoresist, poly(dimethylsiloxane-co-diphenylsiloxane)-modified poly(amic acid) was synthesized to improve the wettability of photoresist. From a study on dynamic contact angles of water, the initial advancing contact angles on poly(dimethylsiloxane)-modified poly(amic acid) and those on poly(dimethylsiloxane-co-diphenylsiloxane)-modified poly(amic acid) are almost the same, but the equilibrium advancing contact angles on poly(dimethylsiloxane-co-diphenylsiloxane)-modified poly(amic acid) are much smaller than those on poly(dimethylsiloxane)-modified poly(amic acid). The decrease in equilibrium advancing contact angles on poly(dimethylsiloxane-co-diphenylsiloxane) appears to indicate migration of phenyl groups to the surface in the polar environment. Thus, photoresist could be wetted on the poly(dimethylsiloxane-co-diphenylsiloxane)-modified poly(amic acid) film. Near-edge X-ray absorption fine structure spectroscopy (NEXAFS) and X-ray photoelectron spectroscopy (XPS) were used to investigate the orientation and surface migration of molecules in poly(dimethylsiloxane-co-diphenylsiloxane).

Keywords: Poly(dimethylsiloxane-co-diphenylsiloxane); poly(amic acid); photoresist; dynamic contact angle; Near-edge X-ray absorption fine structure spectroscopy (NEXAFS); XPS.

*To whom correspondence should be addressed. Tel.: (82-54) 279-2269. Fax: (82-54) 279-8298. E-mail: cep@postech.ac.kr

1. INTRODUCTION

Polyimides have been used as a buffer coating material for semiconductor chips, since these have excellent thermal, mechanical and electrical properties [1, 2]. There have been many studies about the adhesion between polyimide passivation layer and other materials (e.g., epoxy molding compounds (EMCs), SiO_2, copper, Fe–Ni alloy) [3–11]. Siloxane-modified polyimides have also been used to obtain good adhesion strength without use of an adhesion promoter such as silane coupling agents [6–8, 11, 12].

In our previous work [11, 12], we reported that poly(imide-siloxane) containing high-molecular-weight (HMW) poly(dimethylsiloxane) (PDMS) had good adhesion strength to Alloy 42 leadframe. Since the PDMS having low surface energy migrated to the poly(imide-siloxane) surface [13–16], photoresist with high surface energy could not be wetted on the poly(imide-siloxane).

In this study, we synthesized poly(dimethylsiloxane-co-diphenylsiloxane)-modified poly(amic acid) showing good wettability of photoresist. The surface characteristics and chain movements were investigated using dynamic contact angle measurements, near-edge X-ray absorption fine structure spectroscopy (NEXAFS) and X-ray photoelectron spectroscopy (XPS).

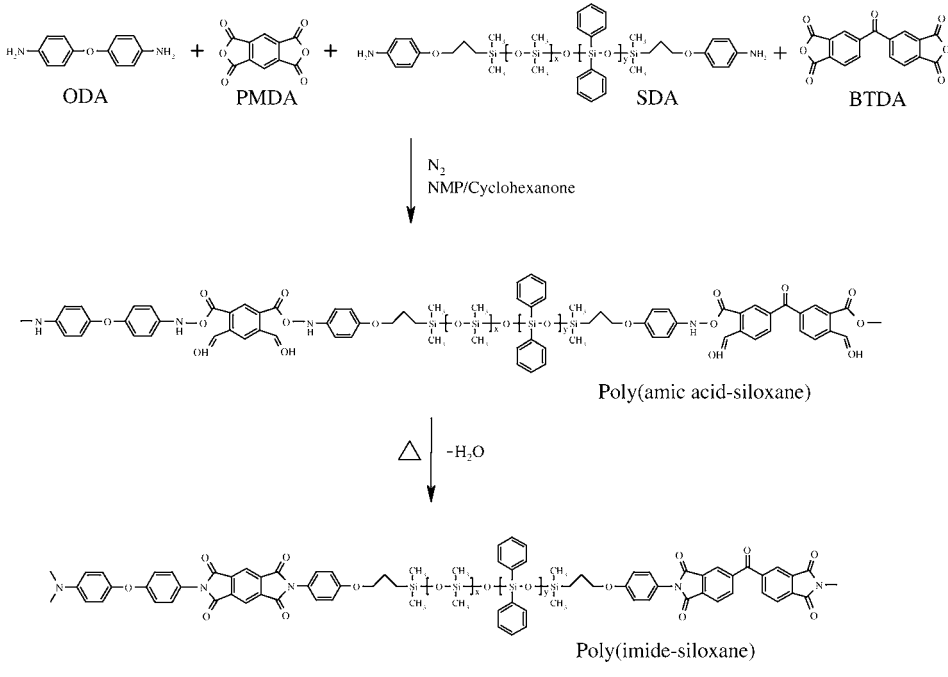

Figure 1. Scheme of synthesis of poly(amic acid-siloxane) and poly(imide-siloxane) from ODA, PMDA, SDA and BTDA.

2. EXPERIMENTAL

2.1. Synthesis of siloxane diamine (SDA) and poly(amic acid-siloxane)

Two kinds of siloxane diamines (SDAs), α,ω-(aminophenoxypropyl)poly(dimethylsiloxane) and α,ω-(aminophenoxypropyl)poly(dimethylsiloxane-co-diphenylsiloxane) were synthesized by ring-opening polymerization of octamethylcyclotetrasiloxane and octaphenylcyclotetrasiloxane (D_4 and D_4^{ph} respectively, United Chemical Technologies, USA) using 1,3-bis(nitrophenoxypropyl)dimethyldisiloxane (BNPPD) both as an initiator and end-blocker [12] (Fig. 1). BNPPD was synthesized as follows: First, potassium *p*-nitrophenoxide was obtained by reaction of *p*-nitrophenol (Aldrich) and potassium hydroxide (Aldrich) at room temperature for 1 h. Then BNPPD was synthesized from potassium *p*-nitrophenoxide and 1,3-bis-(3-chloropropyl)tetramethyldisiloxane (United Chemical Technologies) in N-methylpyrrolidone (NMP, Aldrich) at 110°C for 10 h. The completion of reaction was checked with thin-layer chromatography. BNPPD was recrystallized 3–4 times in 0.3 M KOH aqueous solution. SDAs were synthesized from octamethylcyclotetrasiloxane or octaphenylcyclotetrasiloxane (D_4 or D_4^{ph}) and BNPPD at 110°C for 12 h. Tetramethylammonium hydroxide (TMAH, 25 wt% in methanol), used as a catalyst, was azeotropically distilled. The unused catalyst was decomposed thermally at 150°C for 5 h, and then the unused catalyst and non-reacted cyclics were vacuum-stripped under a pressure of 0.5 mmHg at 160°C for 5 h. The product was reduced with hydrazine (Aldrich) and palladium (Aldrich) to obtain amine end groups. The molecular weights (1500 g/mol) of SDAs were controlled by the ratio of BNPPD to cyclosiloxane (D_4 or D_4^{ph}), and the compositions of SDAs were controlled by the mole ratios of D_4 to D_4^{ph}. For example, the 10 : 0 ratio of D_4 to D_4^{ph} is for α,ω-(aminophenoxypropyl)poly(dimethylsiloxane) and the 7 : 3 ratio of D_4 to D_4^{ph} is for α,ω-(aminophenoxypropyl)poly(dimethylsiloxane-co-diphenylsiloxane).

4,4′-diaminodiphenylether (4,4′-DPE, Wakayama Seika Kogyo, Japan), pyromellitic dianhydride (PMDA, Daicel, Japan), and benzophenone tetracarboxylic dianhydride (BTDA, Daicel) were taken out of bottles in a glove box in an argon atmosphere and used immediately without any purification. Anhydrous N-methylpyrrolidone (NMP, Aldrich) was used as the solvent without further purification, and cyclohexanone (Aldrich), the co-solvent for SDAs, was vacuum-distilled with magnesium sulfate as a dehydrating agent. The details of the synthesis procedure for poly(amic acid-siloxane) were described in previous papers [11–13].

The nomenclature used for poly(amic acid-siloxane) is PI *x*-*y*-MaPb, where *x* and *y* represent molecular weight and content (wt%) of SDA, respectively, and MaPb means the composition of SDA synthesized from the *a* : *b* mol ratio of D_4 to D_4^{ph}. For example, PI 1500-10-M7P3 denotes poly(amic acid-siloxane) having a molecular weight of 1500 g/mol, and 10 wt% of SDA, which was synthesized from a 7 : 3 mol ratio of D_4 to D_4^{ph}.

2.2. Dynamic contact angle measurements

To study the wettability of photoresist (AZ 1511, Clariant), contact angles of water instead of photoresist were measured, because it is difficult to obtain a correct contact angle of photoresist due to its volatility. The spreading coefficient, S, is given as:

$$S = \gamma_{SV} - \gamma_{SL} - \gamma_{LV}, \tag{1}$$

where γ_{SV}, γ_{SL} and γ_{LV} are the solid–vapor, solid–liquid and liquid–vapor interfacial free energies, respectively. When $S > 0$, wetting occurs spontaneously. In our system, γ_{LV} is constant. So, if γ_{SV} increases or γ_{SL} decreases, the photoresist can be wetted well. As the contact angle of water on a solid is inversely proportional to the surface energy of the solid, in an analogous manner we can study the wettability of photoresist with contact angle of water [22]. Advancing and receding contact angles of distilled water on poly(amic acid-siloxane) films were measured using a dynamic contact angle tester (Wet-3000, Rhesca, Japan). The specimens for dynamic contact angle measurements were prepared as follows: aluminum hexahedral plates (dimension: 10 mm width, 40 mm length and 0.31 mm thickness) were cleaned ultrasonically with dichloromethane for 30 min, rinsed with acetone and dried in a convection oven at 80°C for 2 h. Then, these plates were dip-coated with poly(amic acid-siloxane) (solid content 10 wt%) solution and prebaked at 100°C for 1 h.

Dynamic contact angles were calculated using the Wilhelmy plate method as shown in Fig. 2 [14] using the following equation:

$$F = mg + P\gamma_L \cos\theta - F_b, \tag{2}$$

where F is the measured total force, m is the mass of specimen, g is the acceleration of gravity, P is the perimeter of specimen, γ_L is the surface tension of liquid, θ is the contact angle and F_b is the buoyancy force.

For measuring dynamic contact angles, the specimen was dipped into the liquid at a constant velocity of 2 mm/min to a depth of 12 mm below the liquid surface. The contact angle at this point was taken as the initial advancing contact angle. The measured total force on this specimen became constant as a function of immersion time. The constant angle at constant force was taken as the equilibrium advancing angle. Then the specimen was pulled out of the liquid by 4 mm at a rate of 2 mm/min. In the same manner, the initial receding angle and the equilibrium receding angle were measured as shown in Fig. 3. The surface of poly(amic acid-siloxane) was characterized from these four angles.

2.3. Surface characterization of poly(amic acid-siloxane) films using NEXAFS

For NEXAFS studies, poly(amic acid-siloxane)s were spin-coated onto gold-coated silicon wafers (P-type, (100) orientation, Au/Ti/SiO_2/Si wafer, Au 100 nm, Ti 10 nm, SiO_2 300 nm) and pre-baked at 100°C for 1 h. To examine the molecular orientation of poly(amic acid-siloxane) films, two kinds of samples were

$$F = mg + P\gamma_L\cos\theta - F_b$$

F: total force
m: mass of the sample
g: acceleration of gravity
P: perimeter of the sample
γ_L: surface tension of the liquid
θ: contact angle
F_b: buoyancy force

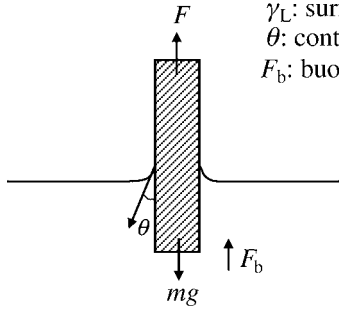

Figure 2. Schematic diagram showing dynamic contact angle measurements using the Wilhelmy method.

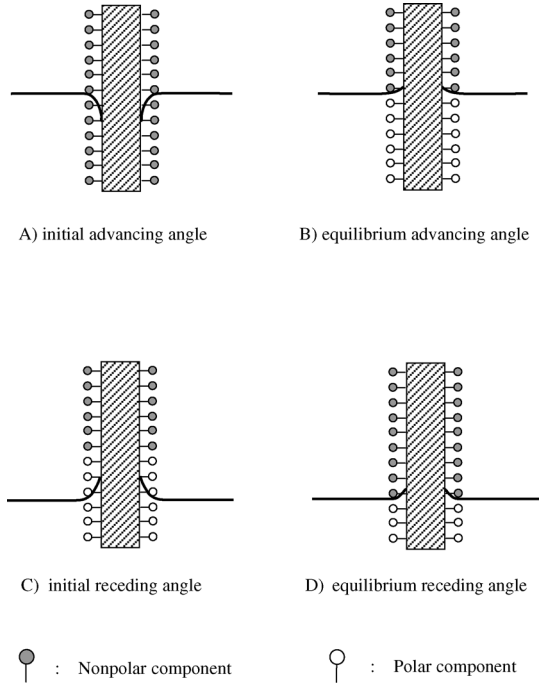

Figure 3. Schematic diagram showing the orientation of molecules at the poly(amic acid-siloxane) surface during dynamic contact angle measurements. Sample is introduced into the water (A and B) and taken out of the water (C and D).

prepared: one was poly(amic acid-siloxane) film on gold-coated silicon wafer for non-polar environment, and the other was a very thin gold (1-nm-thick with discontinuous, cluster-like morphology)-coated poly(amic acid-siloxane) film on gold-coated silicon wafer for polar environment.

Total electron yield (TEY) X-ray absorption experiments were carried out at the 2B1 beam line of Pohang Accelerator Laboratory (PAL) with a resolution of 0.2 eV for both carbon 1s and silicon 2s signals. All spectra were normalized with respect to the electron yield signal from a gold-coated grid reference [17]. The reproducibility of the spectra was checked by multiple scanning. The information depth of the NEXAFS method in the total electron yield mode is estimated to be $\leqslant$10 nm for the C_{1s} signal [18, 19].

To investigate the orientation of siloxane chains in non-polar (vacuum atmosphere) and polar environment (gold), two different angles of incidence of the linearly polarized synchrotron light were used: 90° (electric field vector **E** lies parallel to the surface plane) and 20° (**E** is 70° to the surface plane) [20–24].

2.4. Surface characterization of poly(amic acid-siloxane) films using XPS

The surface atomic composition of poly(amic acid-siloxane) films was investigated by X-ray photoelectron spectroscopy (XPS). The measurements were performed with ESCALAB 220i-XL Photoelectron Spectrometer using a Mg K_α X-ray source (1253.6 eV, 350 W). The high resolution spectra of the sample were recorded and a Gaussian model was used to fit the raw spectra.

The operating pressure during analysis was in the range of 10^{-9} Torr. Angle-resolved XPS measurements were taken at take-off angles of 20° and 90° for both non-polar and polar environments and the sampling depth for a given take-off angle is calculated from equation (3) [25–28],

$$\zeta = 3\lambda \sin\theta, \tag{3}$$

where ζ is the sampling depth, λ is the inelastic mean free path (IMFP) and θ is the take-off angle which is the angle between the detector and the sample surface.

3. RESULTS AND DISCUSSION

3.1. Wettability of photoresist on poly(amic acid-siloxane) film

When photoresist was spin-coated on PI 1500-M10P0 series, photoresist spontaneously dewetted (Table 1). Since PDMS having low surface energy (24 mJ/m^2) migrated to the surface to reduce the surface energy of poly(amic acid-siloxane) (48 mJ/m^2) [11–16]; thus the photoresist having high surface energy could not wet poly(amic acid-siloxane) well [29, 30].

In order to increase the polarity, phenyl groups were introduced into siloxane chains and poly(dimethylsiloxane-co-diphenylsiloxane) was synthesized. Poly(di-

Table 1.
Wettability of photoresist on poly(amic acid-siloxane) films

Sample	SDA composition (mol%)		SDA content in diamine (wt%)	Photoresist behavior
	Poly(dimethyl siloxane)	Poly(diphenyl siloxane)		
PI 1500-1-M10P0	10	0	1	Dewetting
PI 1500-5-M10P0	10	0	5	Dewetting
PI 1500-10-M10P0	10	0	10	Dewetting
PI 1500-20-M10P0	10	0	20	Dewetting
PI 1500-1-M7P3	7	3	1	Wetting
PI 1500-5-M7P3	7	3	5	Wetting
PI 1500-10-M7P3	7	3	10	Wetting
PI 1500-20-M7P3	7	3	20	Wetting

methylsiloxane-co-diphenylsiloxane)-modified poly(amic acid) (PI 1500-M7P3 series) showed good wettability of photoresist (Table 1).

3.2. Dynamic contact angles on poly(amic acid-siloxane) films

Figure 4 shows the initial and equilibrium contact angles on prebaked PI 1500-M10P0 series and PI 1500-M7P3 series in distilled water. In the case of PI 1500-M10P0 series, the initial advancing angles on PI 1500-1-M10P0 and PI 1500-10-M10P0 are 109.4° and 111.2°, respectively. The contact angle of water on pure poly(dimethylsiloxane) (PDMS) is 112°. Thus the surfaces of these samples are almost covered with PDMS even if they had only 1 wt% PDMS (see Fig. 3a).

The equilibrium advancing angles on PI 1500-M10P0 series are smaller than the initial advancing angles. This shows that the surface became more polar than the initial state of contact with water [3]. This originates from the reorientation and migration of PDMS. Since the PDMS not only has polar character due to partial ionic Si−O bond but also possesses a non-polar character due to methyl groups, polar and non-polar groups of flexible PDMS can reorient easily, depending on the polarity of the environment [31, 32]. Also, PDMS can migrate into the bulk to expose polar carboxyl groups of poly(amic acid) in the polar environment (Fig. 3b). With small content of SDA (e.g., when the content of SDA in total diamine is 1 wt%), the PDMS-enriched layer is thin. So, a decrease in equilibrium advancing contact angles can be obtained by the migration of PDMS into the bulk and that of carboxylic groups of poly(amic acid) to the surface. For SDA content higher than 5 wt%, the difference between the initial advancing contact angle and the equilibrium advancing contact angle is reduced.

The initial advancing contact angles on PI 1500-M7P3 series are almost the same as on the PI 1500-M10P0 series and remain unchanged with increasing SDA content. This indicates that the surface of poly(dimethylsiloxane-co-diphenylsiloxane)-modified poly(amic acid) film is covered with PDMS, regardless of incorporation

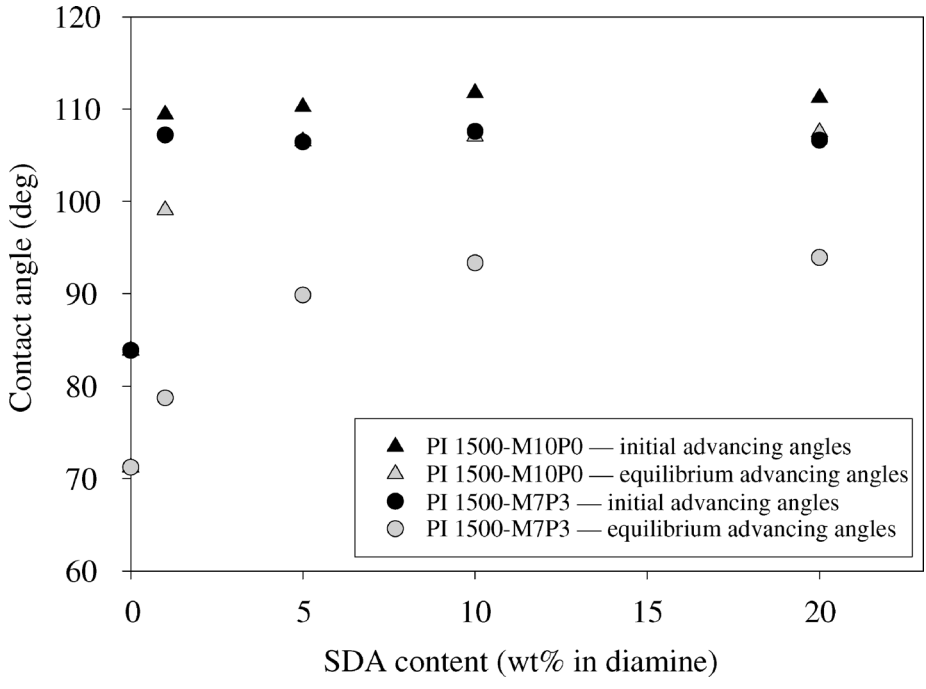

Figure 4. Initial and equilibrium advancing contact angles of water on poly(amic acid-siloxane) films.

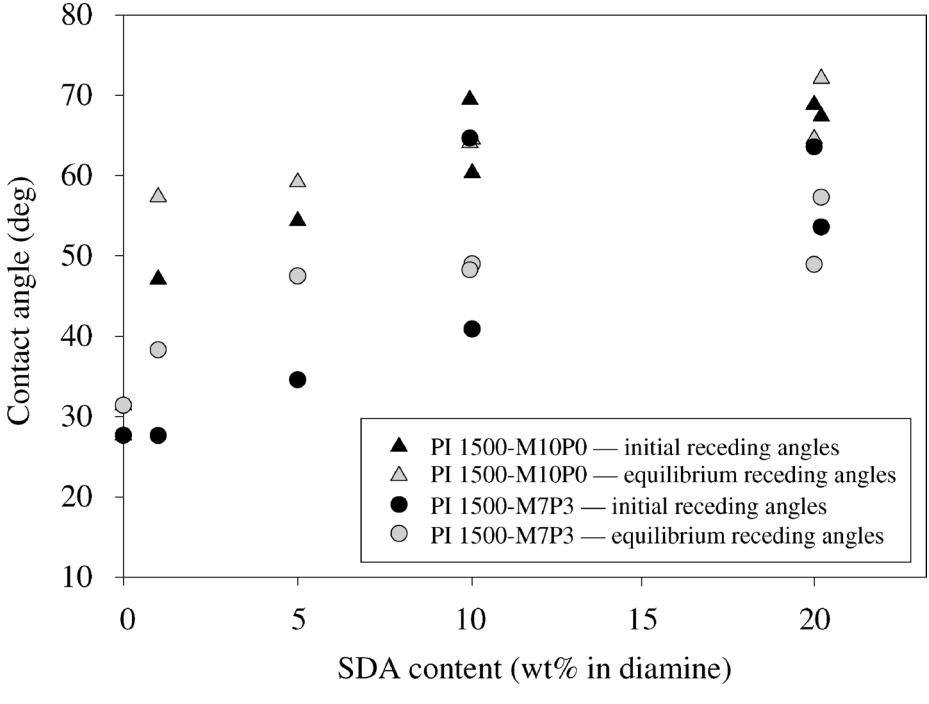

Figure 5. Initial and equilibrium receding contact angles of water on poly(amic acid-siloxane) films.

of poly(diphenylsiloxane) (PDPS) (Fig. 3a). However, the equilibrium advancing contact angles on PI 1500-M7P3 series decrease rapidly. Especially PI 1500-1-M7P3 series shows a very large difference, more than 30°, between the initial advancing contact angle and the equilibrium advancing contact angle. This difference decreases with increase in SDA content. This phenomenon can be explained in the same manner as for PI 1500-M10P0 series. When the environment of the sample changes from non-polar to polar, non-polar groups (methyl groups of PDMS) migrate into the bulk, exposing polar groups (phenyl groups of PDPS) to the surface (Fig. 3b).

The initial receding contact angles on both PI 1500-M10P0 and PI 1500-M7P3 series are smaller than the initial advancing contact angles (Figs 4 and 5). Also the initial receding contact angles on PI 1500-M7P3 series are smaller than those on PI 1500-M10P0 series. This is due to the reorientation of PDMS (Fig. 3c). The equilibrium receding contact angles increased by 5–15° due to the decrease of surface energy of poly(amic acid-siloxane). Non-polar groups (methyl groups), which were hidden in the bulk in the water environment, reoriented and migrated to the surface in the air environment to reduce the interfacial energy between poly(amic acid-siloxane) film and air (Fig. 3d).

3.3. Surface characterization of poly(amic acid-siloxane) films using NEXAFS

Figure 6 shows carbon K-edge NEXAFS spectra of PI 1500-20-M10P0 and PI 1500-20-M7P3. The first five sharp peaks, labeled C1, C2, C3, C4 and C5 at approximately 284.8, 285.4, 286.8, 287.6 and 289.2 eV, respectively, correspond to the π^* bond orbital resonances of carbons as assigned in Table 2 [33–36]. Since the direction of the electric field is parallel to the sample surface with the 90° incident angle [17–22], the smaller resonance peaks for the 90° incident angle, as compared to those for the 20° incident angle, indicate that the π^* bond orbital is normal to the

Table 2.
Assignments of resonance peaks in the carbon NEXAFS spectra for PI 1500-20-M10P0 and PI 1500-20-M7P3

Peak	Photon energy (eV)	Final state
C1	284.8	π^* (C=C, PMDA/BTDA)
C2	285.4	π^* (C=C, ODA, Phenyl)
C3	286.8	π^* (C=C, ODA, Phenyl)
C4	287.6	π^* (C=O, PMDA, BTDA)
C5	289.2	π^* (C=C, ODA, PMDA/BTDA, Phenyl)
C6	290.2	σ^* (C−O, C−Si)
C7	292.2	σ^* (C−O, PMDA/BTDA, Phenyl) σ^* (C−O, ODA), σ^* (C−N)
C8	295.8	σ^* (C=C, ODA, Phenyl)
C9	304.4	σ^* (C=C, ODA, PMDA/BTDA, Phenyl) σ^* (C=O, PMDA, BTDA)

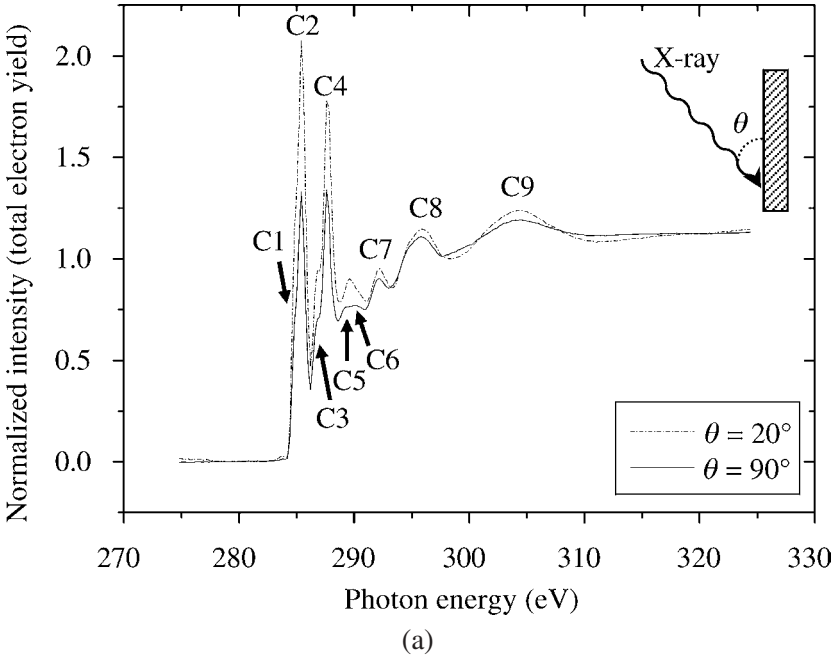

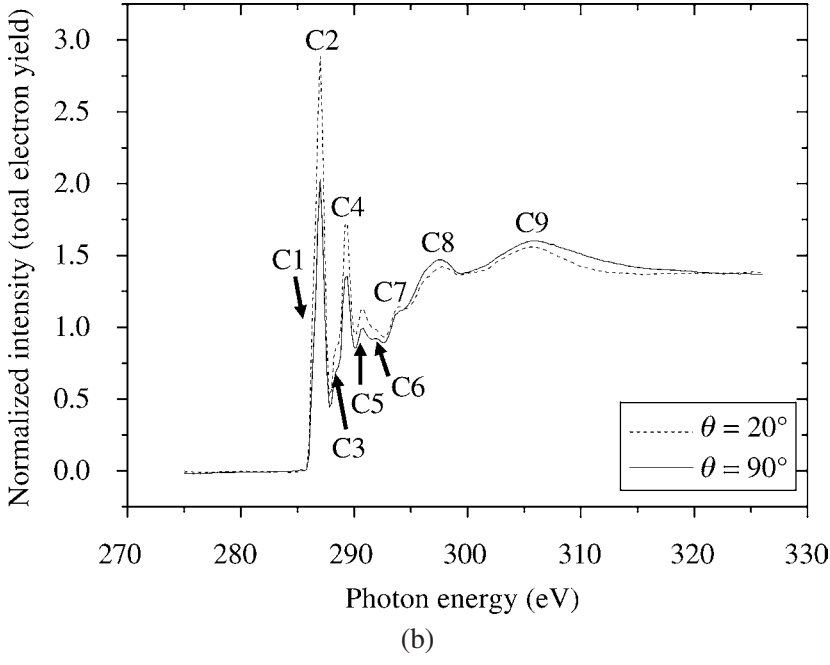

Figure 6. Carbon K-edge total electron yield spectra of (a) PI 1500-20-M10P0 and (b) PI 500-20-M7P3. All spectra were normalized with respect to the electron yield signal from a gold-coated grid reference [17].

Table 3.
Assignments of resonance peaks in the silicon L-edge NEXAFS spectra of PI 1500-20-M10P0 and PI 1500-20-M7P3 in a non-polar environment

Peak	Photon energy (eV)	Final excited state
Si1	102.8	π^* (Si−C_{phenyl})
Si2	104.4	σ^* (Si−C)
Si3	106.0	σ^* (Si−O)
Si4	107.2	σ^* (Si−C)
Si5	108.2	σ^* (Si−C_{phenyl})
Si6	112.8	σ^* (Si−O)

sample surface. This shows that poly(amic acid-siloxane) main chains are oriented parallel to the surface plane.

The peaks labeled C6, C7, C8 and C9 correspond to the σ^* bond orbital resonances for carbons of poly(amic acid-siloxane) as assigned in Table 2. The difference between 20° and 90° incident angles in the σ^* bond orbital resonances is small in contrast to that between 20° and 90° in π^* bond orbital resonances. This is due to co-existence of two kinds of σ^* bond orbitals of C−C and Si−C, and indicates that σ^* bond orbitals align randomly. PI 1500-20-M7P3 shows similar results to PI 1500-20-M10P0 (Fig. 6b). This shows that poly(dimethylsiloxane-co-diphenylsiloxane)-modified poly(amic acid) main chains are also aligned parallel to the sample surface. The C2 peak in Fig. 6b is larger than the C2 peak in Fig. 6a due to the π^* bond orbital resonance of phenyl groups of poly(dimethylsiloxane-co-diphenylsiloxane).

To find out the orientation of methyl and phenyl groups of siloxane at the surface with the polarity of the environment, Si L-edge NEXAFS spectra were recorded as shown in Fig. 7 for PI 1500-20-M10P0 and Fig. 8 for PI 1500-20-M7P3. The peaks labeled Si2 and Si4 are $\sigma*$ bond orbital resonances of Si−C and the peaks labeled Si3 and Si6 are σ^* bond orbital resonances of Si−O (Table 3).

For the case of PI 1500-20-M10P0, the Si2 peak is stronger for 20° than that for 90° incident angle and the Si6 peak is much stronger for 90° than that for 20° in the vacuum (Fig. 7a). Thus, the Si−CH_3 bonds are approximately perpendicular to the surface, and the Si−O bonds are approximately parallel to the surface as illustrated in Fig. 9a in a non-polar environment. For a very thin gold (1 nm thick with discontinuous, cluster-like morphology)-coated poly(amic acid-siloxane), the strengths of Si2 and Si6 peaks at 20° are similar to those at 90° (Fig. 7b). This indicates that methyl groups migrate into the bulk, and siloxane main chain (−O−Si−O−) migrates to the surface in the polar environment, as illustrated in Fig. 9b.

In the case of PI 1500-20-M7P3, the Si3 and Si6 peaks for 20° and 90° incident angles are almost the same in the non-polar environment (Fig. 8a). This indicates that siloxane main chains do not orient parallel to the surface plane, unlike PI 1500-20-M10P0. The Si1 peak, π^* bond orbital resonance of Si-phenyl, for 20°

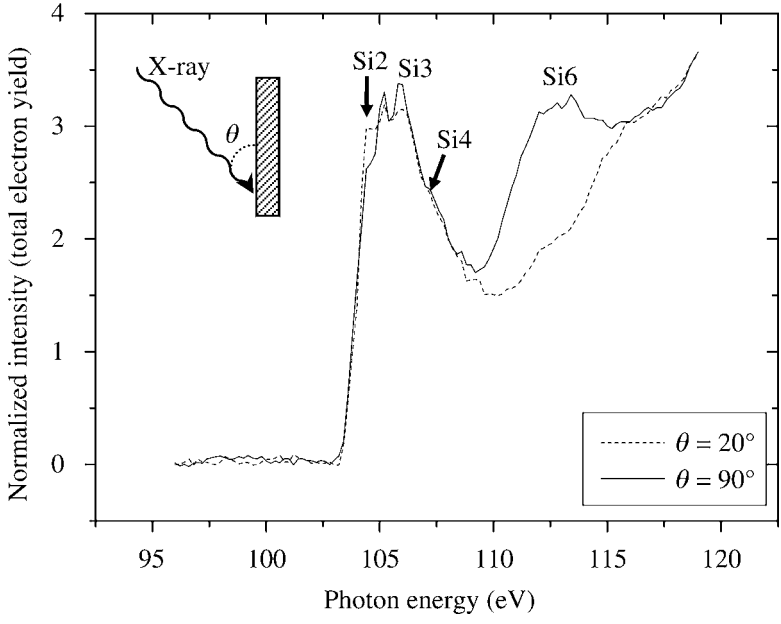

(a)

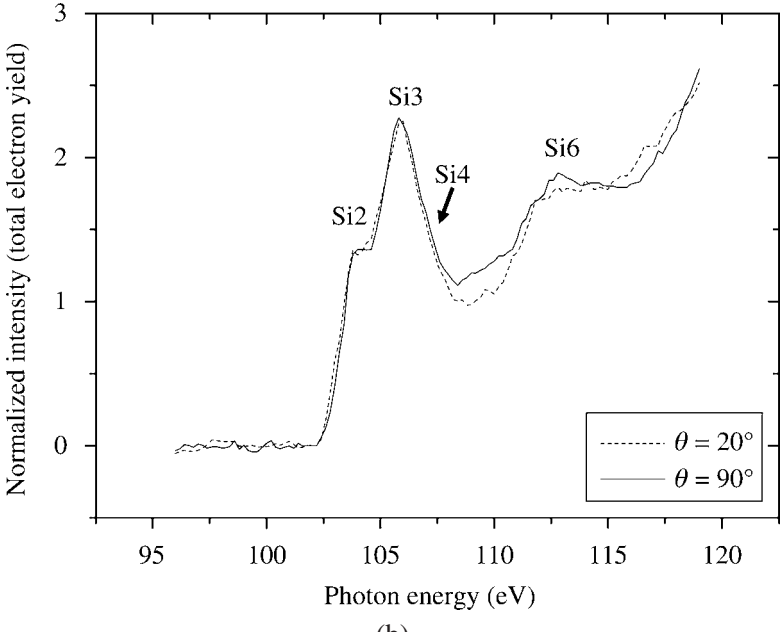

(b)

Figure 7. Silicon L-edge total electron yield spectra of PI 1500-20-M10P0 in (a) non-polar environment and (b) polar environment.

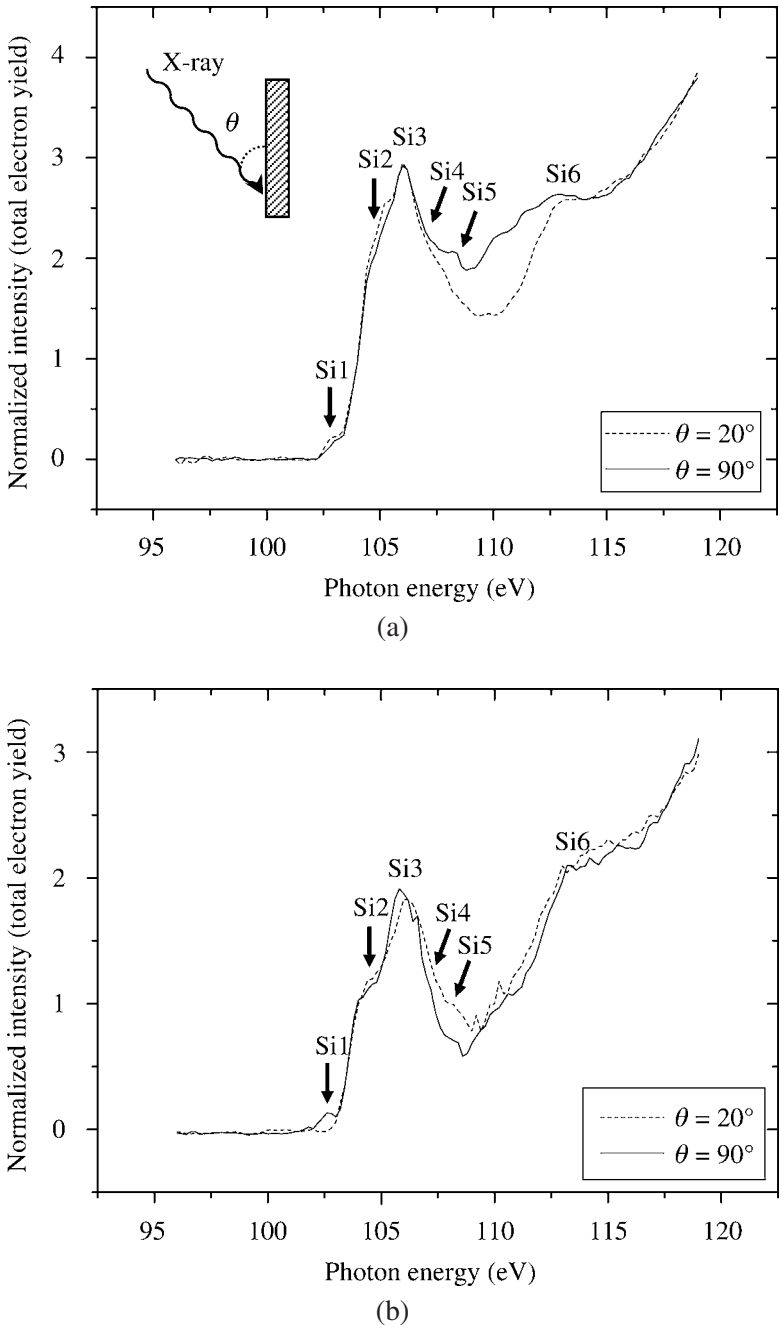

Figure 8. Silicon L-edge total electron yield spectra of PI 1500-20-M7P3 in (a) non-polar environment and (b) polar environment.

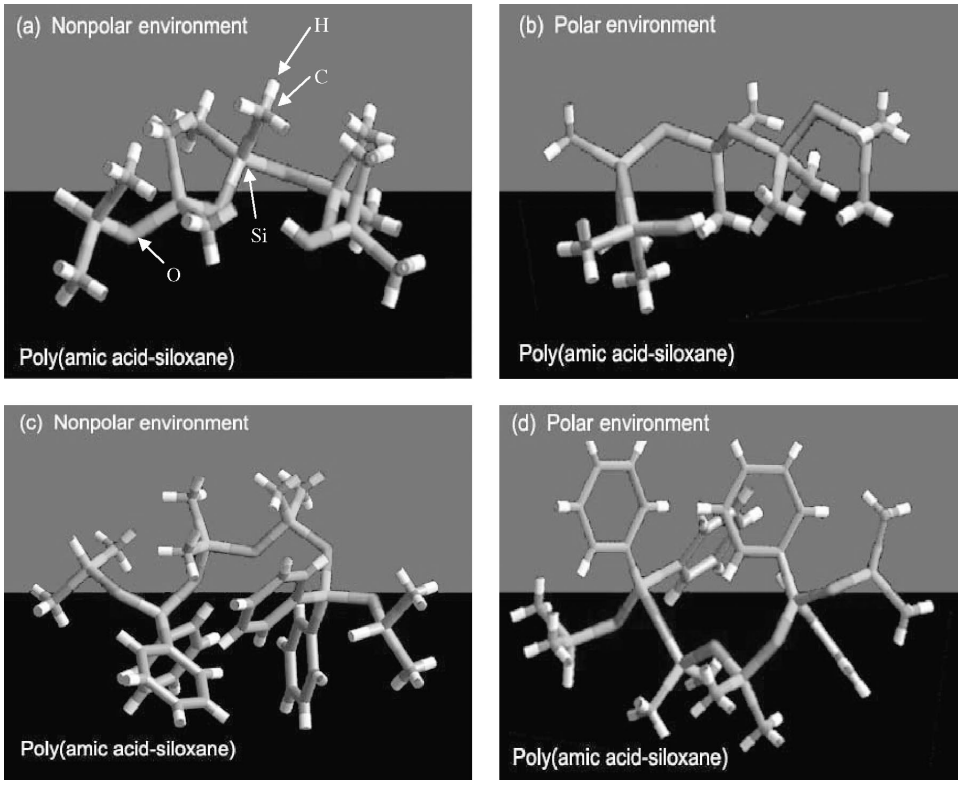

Figure 9. Three-dimensional diagrams showing molecular conformation at poly(amic acid-siloxane) surface. Poly(dimethylsiloxane)-modified poly(amic acid) in (a) non-polar environment and (b) polar environment; poly(dimethylsiloxane-co-diphenylsiloxane)-modified poly(amic acid) in (c) non-polar environment and (d) polar environment.

is slightly stronger than that for 90°, and the Si5 peak, σ^* bond orbital resonance of Si-phenyl, for 90° is stronger than that for 20°. This indicates that phenyl groups are approximately parallel to the surface (as illustrated in Fig. 9c) [37–41].

However, in a polar environment, the Si1 peak for 90° and Si5 peak for 20° are stronger than those for 20° and 90°, respectively. This suggests that the phenyl groups reorient perpendicularly to the surface in order to reduce the interfacial energy, as illustrated in Fig. 9d.

3.4. Surface characterization of poly(amic acid-siloxane) films using XPS

When the take-off angles are 20° and 90°, the sampling depths are about 2.7 nm and about 8 nm, respectively [28]. For both PI 1500-20-M10P0 and PI 1500-20-M7P3 in a non-polar environment, the atomic concentration of Si, originated from siloxane, is larger at the take-off angle of 20° than at 90°, while the atomic concentration of N, originated from amic acid, is larger at the take-off angle of 90° than at 20° (Table 4). This indicates that for both PI 1500-20-M10P0 and

Table 4.
Surface atomic concentrations of PI 1500-20-M10P3 and PI 1500-20-M7P3 in non-polar and polar environments using angle-resolved XPS

Sample	Environment	Take-off angle (°)	Atomic concentration (%)			
			C	O	N	Si
PI 1500-20-M10P0	Non-polar	20	59.1	26.8	2.1	12.0
		90	58.0	30.2	4.5	7.3
PI 1500-20-M10P0	Polar	20	53.8	33.1	2.5	10.6
		90	53.6	34.0	5.0	7.3
PI 1500-20-M7P3	Non-polar	20	54.4	32.3	2.3	11.0
		90	67.4	22.1	5.0	5.5
PI 1500-20-M7P3	Polar	20	56.3	31.4	2.6	9.7
		90	60.0	30.2	5.9	3.9

PI 1500-20-M7P3, there is a siloxane-enriched layer at the surface in a non-polar environment [11, 13]. Also, the surface atomic concentration of Si reduced and that of N increased in a polar environment. This indicates that, in a polar environment, siloxane (PDMS) migrates into the bulk in order to reduce the interfacial energy in a polar environment. Because PI 1500-20-M10P0 has a thick, about 10 nm, PDMS-enriched layer [13], all PDMS cannot reside in the bulk and it, thus, showed high contact angle of water, while PI 1500-20-M7P3 has a lower concentration of siloxane (PDMS and PDPS) at the surface and, thus, showed smaller contact angle of water due to exposure of PDPS at the surface after migration of PDMS into the bulk in a polar environment.

4. CONCLUSIONS

When photoresist was spin-coated on poly(dimethysiloxane)-modified poly(amic acid) (PI 1500-M10P0 series), photoresist spontaneously dewetted due to its low surface energy. However, poly(dimethylsiloxane-co-diphenylsiloxane)-modified poly(amic acid) (PI 1500-M7P3 series) showed a good wettability of photoresist. From the study of dynamic contact angles in water, the initial advancing angles on poly(dimethylsiloxane)-modified poly(amic acid) and poly(dimethylsiloxane-co-diphenylsiloxane)-modified poly(amic acid) are almost the same, but the equilibrium advancing contact angles on poly(dimethylsiloxane-co-diphenylsiloxane)-modified poly(amic acid) are much smaller than those on poly(dimethylsiloxane)-modified poly(amic acid). The decrease in equilibrium contact angle on poly(dimethylsiloxane-co-diphenylsiloxane) is due to the migration of phenyl groups to the surface in the polar environment. Spectroscopically we observed the orientation and migration of siloxane using Si L-edge NEXAFS and XPS.

Acknowledgements

This work was supported by the Korea Research Foundation Grant (KRF-2002-005-D00008).

REFERENCES

1. H. Satou, H. Suzuki and D. Makino, in: *Polyimides*, D. Wilson, H. Stenzenberger and P. M. Hergenrother (Eds), p. 242. Blackie & Sons, New York, NY (1993).
2. C. Feger and H. Franke, in: *Polyimides: Fundamentals and Applications*, M. K. Ghosh and K. L. Mittal (Eds), p. 759. Marcel Dekker, New York, NY (1996).
3. L. P. Buchwalter, *J. Adhesion Sci. Technol.* **4**, 697 (1990).
4. D. Suryanarayana and K. L. Mittal, *J. Appl. Polym. Sci.* **30**, 3107 (1985).
5. H. G. Linde, *J. Polym. Sci. Polym. Phys.* **26**, 1149 (1988).
6. T. H. Yoon, C. A. Arnold-McKenna and J. E. McGrath, *J. Adhesion* **39**, 15 (1992).
7. H. K. Yun, K. Cho, J. H. An, C. E. Park, S. M. Sim and J. M. Park, *J. Adhesion Sci. Technol.* **8**, 1395 (1994).
8. K. W. Lee, G. F. Walker and A. Viehbeck, *J. Adhesion Sci. Technol.* **9**, 1125 (1995).
9. G. C. Tesoro, G. P. Rajendran, C. E. Park and D. R. Uhlmann, *J. Adhesion Sci. Technol.* **1**, 39 (1987).
10. J. H. Seo, J. H. Kang, K. Cho and C. E. Park, *J. Adhesion Sci. Technol.* **16**, 1839 (2002).
11. J. H. Kang, K. Cho and C. E. Park, *Polymer* **42**, 2513 (2001).
12. J. H. Kang, K. Cho and C. E. Park, *J. Adhesion Sci. Technol.* **15**, 913 (2001).
13. C. K. Cho, J. H. Kang, Y. T. An, K. Cho, C. E. Park and W. Huh, *J. Adhesion Sci. Technol.* **14**, 108 (2000).
14. S. Wu, *Polymer Interface and Adhesion*. Marcel Dekker, New York, NY (1982).
15. N. L. Jarvis, R. B. Fox and W. A. Zismn, *Adv. Chem. Ser.* **43**, 317 (1964).
16. M. K. Bernett, *Polym. Eng. Sci.* **17**, 450 (1977).
17. N. Sprang, D. Theirich and J. Engemann, *Surf. Coating. Technol.* **74**, 689 (1995).
18. A. Lippitz, J. F. Friedrich, W. E. S. Unger, A. Schertel and Ch. Wöll, *Polymer* **37**, 3151 (1996).
19. A. Lippitz, I. Koprinarov, J. F. Friedrich, W. E. S. Unger and Ch. Wöll, *Polymer* 3**7**, 3157 (1996).
20. J. Stöhr, *NEXAFS Spectroscopy; Springer Series in Surface Science 25*. Springer, Berlin (1992).
21. R. A. Rosenberg, P. J. Love and V. Rehn, *Phys. Rev. B* **33**, 4034 (1986).
22. I. Koprinarov, A. Lippitz, J. F. Friedrich, W. E. S. Unger and Ch. Wöll, *Polymer* **39**, 3001 (1998).
23. D. G. J. Sutherland, J. A. Carlisle, P. Elliker, G. Fox, T. W. Hagler, I. Jimenez, F. J. Himpsel, D. K. Shuh, W. M. Tong, J. J. Jia, T. A. Callcott and D. L. Ederer, *Appl. Phys. Lett.* **68**, 2046 (1996).
24. T. Sakai, K. Ishikawa, H. Takezoe, N. Matsuie, Y. Yamamoto, H. Ishii, Y. Ouchi, H. Oji and K. Seki, *J. Phys. Chem. B* **105**, 9191 (2001).
25. C. M. Chan, *Polymer Surface Modification and Characterization*. Hanser, Münich (1994).
26. C. Jama, J. D. Quensierre, L. Gengembre, V. Mineau, J. Grimblot and O. Dessaux, *Surf. Interf. Anal.* **27**, 653 (1999).
27. C. M. Chan, T. M. Ko and H. Hiraoka, *Surface Sci. Rep.* **24**, 1 (1996).
28. Q. T. Le, J. J. Pireaux and R. Caudano, *J. Adhesion Sci. Technol.* **11**, 735 (1997).
29. W. J. Ort, J. H. van Zanten, W. Wu and S. K. Satija, *Phys. Rev. Lett.* **71**, 867 (1993).
30. S. Wu, in: *Polymer Blends,* D. R. Paul and S. Newman (Eds), p. 244. Academic Press, New York, NY (1978).
31. H. Yasuda, T. Okuno and K. Yoshida, *J. Polym. Sci. Polym. Phys.* **26**, 1781 (1998).
32. E. G. Rochow and H. G. Leclair, *J. Inorg. Nucl. Chem.* **1**, 92 (1955).

33. M. G. Samart, J. Stöhr, H. R. Brown, T. P. Russell, J. M. Sands and S. K. Kumar, *Macromolecules* **29**, 8334 (1996).
34. K. Weiss, C. Wöll, E. Böhm, B. Fiebranz, G. Forstmann, B. Peng, V. Scheumann and D. Johannsmann, *Macromolecules* **31**, 1930 (1998).
35. J. Stöhr, M. G. Samart, A. Cossy-Favre, J. Diaz, Y. Momoi, S. Odahara and T. Nagata, *Macromolecules* **31**, 1942 (1998).
36. K. Weiss, C. Wöll and D. Johannsmann, *J. Chem. Phys.* **113**, 11297 (2000).
37. J. Zhao, S. R. Rojstaczer, J. Chen, M. Xu and J. A. Gardella, *Macromolecules* **32**, 455 (1999).
38. K. Seki, H. Ishii, A. Yuyama, M. Watanabe, K. Fukui, E. Ishiguro, J. Yahazaki, S. Hasegawa, K. Horiuchi, T. Ohta, H. Isaka, M. Fujino, M. Fujiki, K. Furukawa and N. Matsumoto, *J. Electron. Spectrosc. Relat. Phenom.* **78**, 403 (1996).
39. G. U. Stephen, C. T. Turci, T. Tyliszczak, M. A. Brook and A. P. Hitchcock, *Organometallics* **16**, 2080 (1997).
40. V. R. McCrary, F. Sette, C. T. Chen, A. J. Lovinger, M. B. Robin, J. Stöhr and J. M. Zeigler, *J. Chem. Phys.* **88**, 5925 (1988).
41. J. M. Zeigler and F. W. G. Fearon, *Silicon-based Polymer Science: A Comprehensive Resource*. American Chemical Society, Washington, DC (1990).